AIAA-92-4455-CP

REENTRY CONTROL OF A LOW-LIFT MANEUVERABLE SPACECRAFT

Axel J. Roenneke* and Klaus H. Well†
Institute of Flight Mechanics and Control, University of Stuttgart, Germany

Abstract

Commercial operation of space laboratories will rely on small, unmanned reentry capsules to retrieve experimental products independent from Shuttle services. An example for such a concept is the Space Mail system studied by the European Space Agency. This paper presents a trajectory control system based on linear state feedback to guide and control the reentry glide of low-lifting capsules. A technique to design a time-varying controller is derived and applied. Simulation results of spatial flights over a rotating earth show that the designed controller effectively responds to entry condition offsets on several reference trajectories. Also, the controller is capable of tolerating modified vehicle parameters as well as atmospheric disturbances, and the same controller gain functions are successfully applied to different reference trajectories.

Nomenclature

$\mathbf{A}(t)$	Full order plant matrix
$\mathbf{A}_r(t)$	Reduced-order plant matrix
$\mathbf{B}(t)$	Full order control matrix
$\mathbf{B}_r(t)$	Reduced-order control matrix
$\mathbf{F}(t)$	Feedback gain matrix
$\mathbf{P}(t_k)$	Solution of the algebraic Riccati eq.
$\mathbf{Q}$	Diagonal weighting matrix
$\mathbf{x}(t)$	State vector
$\delta\mathbf{x}(t)$	State error vector
$\delta\mathbf{x}_r(t)$	Reduced-order state error vector
C_D	Drag Coefficient
C_L	Lift Coefficient
D	Drag force
g	Acceleration of gravity
$g_\circ$	Acceleration of gravity at sea level
L	Lift force
m	Mass of vehicle
n_G	Aerodynamic load factor
r	Distance from planet's center of gravity
$r_\circ$	Radius of the Earth
S	Reference area on vehicle
t	Flight time
v	Vehicle's relative speed
γ	Flight path angle
ε	Lift-to-drag ratio, C_L/C_D
θ	Geodetic longitude
ρ	Atmospheric density
$\rho_\circ$	Atmospheric density at sea level
σ	Bank angle
ϕ	Geodetic latitude
ψ	Heading angle

Introduction

To operate laboratories in space efficiently, small unmanned reentry vehicles have been suggested to retrieve experimental products independent from Shuttle services. These cargo carriers shall be readily available and inexpensive to use, yet safe for delicate payload and easy to recover. An example for such a concept is the Space Mail system studied by the European Space Agency[1].

On its reentry mission (see Fig. 1), the Space Mail capsule is jettisoned from the space station in low-earth orbit of 500 km altitude and −28.5 degrees inclination. After a deorbit maneuver, the capsule goes into a Keplerian transfer orbit and reaches the detectable atmosphere at 120 km altitude with an entry speed of approximately 7900 meters per second relative to the rotating earth. This is the interface condition to atmospheric reentry. The capsule then passes through the atmosphere on a gliding path. An on-board guidance, navigation, and control system is desired to limit drag deceleration and to steer the capsule closer to the landing site. The final approach phase begins when the vehicle is parachuted from an altitude of 5 km to the ground[1,2].

In the original configuration used here, the Space Mail reentry module is designed as a slender cone

*Graduate Student, Member AIAA.
†Professor, Member AIAA.

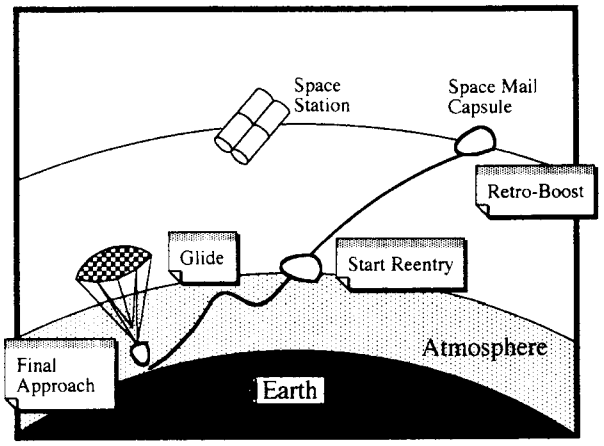

Figure 1: Space Mail mission scenario. The capsule is jettisoned in low-earth orbit and reaches the atmosphere on a Keplerian transfer orbit.

with a spherical nose cap[1]. The base diameter is 0.5 meters and the overall height is 0.8 meters. The total mass is estimated at 80 kg. To provide aerodynamic lift, one side of the cone is flattened, resulting in a constant hypersonic lift-to-drag ratio of about 0.5. Several modified configurations have been investigated in Ref. 2. The capsule's attitude can be changed by moving the center of gravity, for example, via a servo-controlled ballast mass. By changing the direction of the lift vector, the vehicle is thus capable of maneuvering in the atmosphere[1].

A guidance and control system for the Space Mail capsule faces problems similar to those of the Gemini and Apollo missions[3,4], except for the smaller size and mass of the vehicle. A simple, yet reliable control system must restrict the vehicle to a flight path inside the load limits even under adverse conditions. The control system must respond to off-nominal entry conditions and must be tolerant to aerodynamic uncertainties and atmospheric disturbances. Finally, the system must function autonomously without ground or pilot control.

In the past, reentry guidance has been built upon a combination of two different strategies: path following (when the controller tries to reach a predetermined trajectory) and path prediction (when the controller computes a new trajectory in advance based on the actual flight conditions). Clearly, path prediction is a more versatile tool than path following, which is limited by the available number of reference trajectories. Predictors are more flexible to changing entry conditions and vehicle parameters. However, they may require excessive real-time computations and more hardware aboard the spacecraft than path followers. Therefore, previously implemented controllers have been a combination of the two methods. The Gemini guidance system[4] predicts the reentry trajectory analytically based on pre-entry conditions and determines the necessary open-loop control input; after the beginning of reentry, a controller modifies this desired control input as to limit drag deceleration. The Space Shuttle reentry guidance system[5] is based on a nominal drag deceleration versus velocity profile and consists of two loops. The inner loop controls the drag deceleration via bank angle commands, the outer loop adjusts the nominal drag profile in order to match the analytically predicted downrange with the desired.

Self-reliant predictor methods have been suggested for low-lifting vehicles, such as the Inertial Upper Stage vehicle[6] as well as the Space Mail capsule[2]. To determine the control input, these systems use numerical fast-time integration of (simplified) equations of motion, based on the current flight conditions during reentry. Eventually, this technique may be combined with optimization procedures[6,7] to select a desired trajectory from performance criteria such as peak deceleration and total heat load. However, the required hardware for such schemes, based on current technology standards, is regarded as too bulky and heavy to be feasible for implementation in a Space Mail-type vehicle.

Instead of simplifying predictive schemes to make them applicable for small capsules, the concept presented in this paper is a guidance system based on path following[3,8]. We propose reentry guidance for the Space Mail capsule using a reference trajectory defined by altitude, velocity, and flight path angle versus time. Once the vehicle is close enough to the expected entry conditions, a controller locks onto the desired path. This concept requires a minimum of navigation and control hardware. The disadvantages of this scheme – less flexibility to changing entry conditions and flight parameters – are counteracted by the design of a multivariable, time-varying state feedback controller. The control system is designed to respond to off-nominal entry conditions and to compensate for uncertainties in the vehicle's aerodynamic properties and atmospheric dis-

turbances.

State feedback is a feasible design approach, since current flight conditions may be obtained at any time from satellite navigation receivers in addition to conventional inertial measurement units (IMU's) aboard the spacecraft. Receivers for the Navstar Global Positioning System (GPS) for use in spacecraft are available with a total mass of 6 kg and the size of a car stereo[9]. Position and velocity are ascertained at a sample rate of 200 Hertz with an accuracy of ±30 meters and ±0.3 meters per second, respectively, even if the spacecraft is moving at orbital speeds. Integrated systems, cross-filtering GPS and IMU information for higher accuracy, are under development and have been successfully used for autonomous approach and landing of aircraft[10].

The control system design applied to the Space Mail trajectory is based on several linearized system models derived from a non-linear set of equations of motion. The feedback gain functions are calculated using Linear Quadratic Regulator (LQR) optimization. This design scheme and the exact mathematical system model have been presented in a previous paper[11]. The preliminary simulation results presented there show that such a controller effectively responds to entry speed offsets of up to ±5 per cent. In this paper, the control system performance is investigated using realisitic entry condition dispersions of several states. Simultaneously, the control system is submitted to varying aerodynamic and atmospheric parameters. Lastly, it is evaluated how the same gain functions perform on reference trajectories different from the trajectory for which the gains are designed.

State Space System Model

In order to describe a space vehicle returning to the surface of a rotating earth, the following model assumptions are made: the vehicle is a point in space with constant mass; the earth is a sphere, rotating with a constant angular velocity; the forces acting on the vehicle are gravity, aerodynamic lift, and drag; earth winds, when compared to the horizontal velocity of the vehicle, can be ignored, such that the vehicle's ground and air speed are identical; the earth has a Newtonian gravity field whose center coincides with the geometric center of the globe; and the local gravitational acceleration is unaffected by the mass of the vehicle.

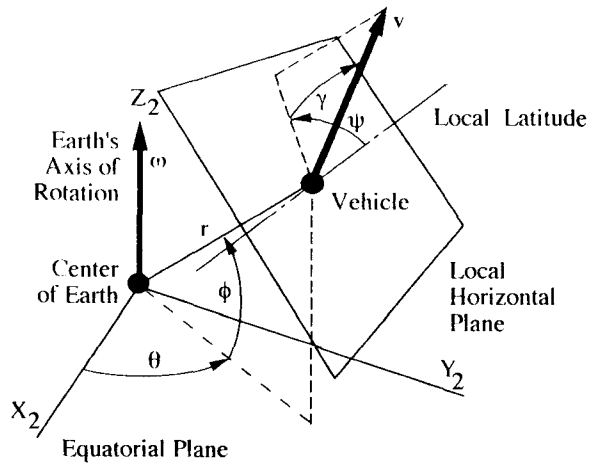

Figure 2: Definition of state variables with respect to the earth-fixed reference frame. The local horizontal plane is perpendicular to the position vector, $\vec{r}$. The X_2 and Y_2 axes are contained in the earth's equatorial plane, the Z_2 axis is aligned with the earth's axis of rotation.

In state space form, the equations of motion for a spatial flight are functions of six state variables defined in Earth-fixed coordinates as shown in Fig. 2. These definitions are consistent with standard literature[12,13]. The position of the vehicle is described by the states (r, θ, ϕ), where r is the distance from the center of the earth, while θ and ϕ are geodetic longitude and latitude. States (v, γ, ψ) specify the velocity vector, where v is the vehicle's ground speed, and the angles γ and ψ give the direction. The flight path angle, γ, is formed by the velocity vector and the local horizontal plane and is positive for ascent. The heading angle, ψ, is measured with respect to the local latitude.

The direction of the lift vector is measured with respect to the local vertical plane that is spanned by the vehicle's position and velocity vectors. The lift vector and the local vertical plane form the velocity bank angle, σ, which is the system. Since the vehicle is modeled as a point mass, the dynamics of a rolling maneuver are disregarded in this analysis. Changes in bank angle are assumed to be instantly attainable.

The mathematical system model in terms of the state variables defined above is based on the equations for a point mass moving over a rotating earth. These equations can be found in Ref. 13 and, in the dimensionless form used here, in Ref. 11. For the

following treatment, it is sufficient to view them as a system of six non-linear, autonomous state equations which can be abbreviated to

$$\dot{\mathbf{x}} = \mathbf{f}(\mathbf{x}, \sigma) \tag{1}$$

where the state vector, $\mathbf{x}(t)$, comprises the six state variables defined above:

$$\mathbf{x}(t) = [\, r \; v \; \gamma \; \theta \; \phi \; \psi \,]^T \tag{2}$$

The state equations are coupled internally by the aerodynamic lift and drag forces, L and D, which are, in this model, related to the speed, v, and

$$L = \frac{1}{2} C_L \rho(r) S v^2 \tag{3}$$

$$D = \frac{1}{2} C_D \rho(r) S v^2 \tag{4}$$

For the Space Mail capsule, the aerodynamic surface, S, is 0.9 square meters, the lift-to-drag ratio, $\varepsilon = C_L/C_D$, is 0.52 in hypersonics, the drag coefficient, C_D, is 0.35, and the mass is estimated at 80 kilograms[1]. These vehicle parameters are assumed to be constant but bearing uncertainties.

The load factor, n_G, is defined as the magnitude ratio of the resulting aerodynamic forces, $\vec{L} + \vec{D}$, to the weight of the vehicle, $m\,\vec{g}$. Using the definitions of L and D in Eqs. (3,4) and assuming a Newtonian gravity law, $g = g_\circ (r_\circ / r)^2$, the load factor can be written as:

$$n_G = \frac{S C_D \sqrt{1+\varepsilon^2}}{2\, g_\circ\, r_\circ^2\, m} \; \rho(r)\, r^2\, v^2 \tag{5}$$

Eq. (5) shows that the aerodynamic deceleration depends only on the (r, v) path of the vehicle's trajectory. To limit the maximum value of n_G, it is necessary to control the trajectory within the altitude-velocity plane.

Trajectory Control Concept

The guidance method we propose for the Space Mail capsule uses the principle of a reference trajectory. A path controller is used to follow this desired path. How the reference path is obtained – by a particular guidance law or an optimization procedure – does not affect the control concept and is not subject of this paper. The perturbation guidance scheme is a well-known method[8,14] and has been considered for reentry guidance since the 1960s[3]. It is the goal of current research to investigate whether such a scheme is also applicable to future European low-lifting spacecraft, such as the Space Mail system[15].

If the path controller design is based on the trajectory error with respect to the reference, the reentry control problem is stated as a classical multivariable tracking problem. For low-lifting vehicles, reentry trajectories are slowly varying[3], which can be shown in particular for the Space Mail system[16]. Thus, a linear regulator is capable of tracking the reference path. This design approach is summarized in the following, more details are given in Ref. 11.

Using linear feedback of the state errors, the controller continuously adjusts the bank angle, which represents the control input to the capsule model. Given that reentry begins under off-nominal entry conditions, the controller effectively corrects the actual trajectory to match the reference.

For the controller design, a linearized system is defined with respect to the trajectory error. Let $\mathbf{x}_R(t)$ and $\sigma_R(t)$ denote the state and control histories of the reference trajectory, respectively. For small deviations $\delta\mathbf{x} = \mathbf{x} - \mathbf{x}_R$ and $\delta\sigma = \sigma - \sigma_R$ the state equations can be written in linear form as

$$\delta\dot{\mathbf{x}} = \mathbf{A}(t)\delta\mathbf{x} + \mathbf{B}(t)\delta\sigma \tag{6}$$

where the plant matrix, $\mathbf{A}(t)$, and the control matrix, $\mathbf{B}(t)$, are given by:

$$\mathbf{A}(t) = \left.\frac{\partial \mathbf{f}}{\partial \mathbf{x}}\right|_R ; \qquad \mathbf{B}(t) = \left.\frac{\partial \mathbf{f}}{\partial \sigma}\right|_R \tag{7}$$

Since the system and control matrices, $\mathbf{A}(t)$ and $\mathbf{B}(t)$, vary with time, it is necessary to compute a time-varying feedback gain schedule. However, to do so, $\mathbf{A}(t)$ and $\mathbf{B}(t)$ need not be treated as true functions of time. As shown in Ref. 11, it is sufficient to evaluate $\mathbf{A}(t)$ and $\mathbf{B}(t)$ only at discrete times, t_k. At each t_k the design is repeated for a locally time-invariant system with constant matrices $\mathbf{A}(t_k)$ and $\mathbf{B}(t_k)$. These linear system and control matrices are obtained numerically along a reference trajectory with a time increment of two seconds over a control time interval of 600 seconds after beginning of reentry. Typical numerical values for a linearized Space Mail system are listed in Table 1.

A desirable reference path, for example to limit the maximum aerodynamic deceleration, is mainly concerned with the trajectory in the (r, v) plane. To control these states, the linear system model can be reduced to a system of three states (r, v, γ). It

Table 1: Linear system and control matrices 200 seconds after reentry at about 60 km altitude and a velocity of 6000 meters per second on a trajectory with constant 45 degrees bank angle . The numerical values are based on the Space Mail capsule with a lift-to-drag ratio of 0.52, a mass of 80 kg, and an aerodynamic surface of 0.9 m^2.

$\mathbf{A}(t=200)$						$\mathbf{B}(t=200)$
r	v	γ	θ	ϕ	ψ	σ
0	1.1512e–05	9.6508e–04	0	0	0	0
1.9628e+00	–6.2927e–03	–1.2150e–03	0	3.8631e–08	–1.7966e–06	0
–9.2661e–01	4.7312e–03	–5.5669e–06	0	–7.3366e–05	–3.8757e–06	–1.1569e–03
–1.0730e–03	1.3943e–03	–1.0047e–05	0	5.7928e–04	–3.2481e–05	0
2.8374e–05	–3.6869e–05	2.6568e–07	0	0	9.5540e–04	0
–9.2831e–01	8.3448e–04	1.1590e–05	0	–1.3602e–03	–1.4193e–05	1.1569e–03

is these three states that exactly determine deceleration and heat load during reentry[11,16]. Hence, even for a system with weak connectivity, reentry trajectory control based on state feedback is a feasible concept. The reduced-order system linear system, comprising the reduced-order states $\delta\mathbf{x}_r = [\delta r,\ \delta v,\ \delta\gamma]^T$ is given by:

$$\delta\dot{\mathbf{x}}_r = \mathbf{A}_r(t)\delta\mathbf{x}_r + \mathbf{B}_r(t)\delta\sigma \tag{8}$$

For the controller design, the reduced-order matrices $\mathbf{A}_r(t)$ and $\mathbf{B}_r(t)$ are approximated by the corresponding submatrices of $\mathbf{A}(t_k)$ and $\mathbf{B}(t_k)$ as indicated in Table 1. At each discrete time t_k, a linear control law is suggested of the form

$$\delta\sigma = -\mathbf{F}(t_k)\,\delta\mathbf{x}_r \tag{9}$$

where the feedback gains, $\mathbf{F}(t_k)$, are constants. These gain constants are obtained by minimizing an infinite-horizon quadratic performance criterion

$$\lim_{t_f\to\infty} \int_0^{t_f} (q_1\,\delta r^2 + q_2\,\delta v^2 + q_3\,\delta\gamma^2 + q_\sigma\,\delta\sigma^2)dt \tag{10}$$

with constant non-negative weighting coefficients, q_i, on state and control errors. This problem is referred to as Linear Quadratic Deterministic Regulator optimization[17] (LQR). If the system is controllable, the feedback gains, F(tk), are given by

$$\mathbf{F}(t_k) = \frac{1}{q_\sigma}\,\mathbf{B}_r^T(t_k)\mathbf{P}(t_k) \tag{11}$$

The constant symmetric matrix $\mathbf{P}(t_k)$ is found as the solution of the Algebraic Riccati Equation (ARE) which is given by:

$$0 = \mathbf{Q} - \mathbf{P}\mathbf{B}_r\frac{1}{q_\sigma}\mathbf{B}_r^T\mathbf{P} + \mathbf{P}\mathbf{A}_r + \mathbf{A}_r^T\mathbf{P} \tag{12}$$

The diagonal matrix $\mathbf{Q}$ is given by the weighting coefficients, numerical values of which have been chosen using Bryson's rule[14]:

$$\begin{aligned}\mathbf{Q} &= \text{diag}\,(q_1,\ q_2,\ q_3)\\ &= \text{diag}\,(1,\ 0.1,\ 10)\end{aligned} \tag{13}$$

If the system is controllable, the state feedback control law is asymptotically stable, and the solution $\mathbf{P}(t_k)$ of the associated ARE can be obtained using the method of diagonalization[17,18].

With the above weighting coefficients, the LQR design is repeated at the same discrete times t_k at which the system is linearized. The resulting feedback gains, $\mathbf{F}(t_k)$, consist of the gains on altitude error, on velocity error, and on flight path angle error. A typical gain schedule calculated for a trajectory with constant 45 degrees bank angle and nominal entry conditions is shown in Fig. 3.

It is the key hypothesis of the proposed controller design that the sequence of discrete gain constants can be interpolated over time and used collectively as a continuous gain function to control the time-varying system. In the simulation, the time increment of the discrete gain values is two seconds over a time interval from 0 to 600 seconds. After 600 seconds, the controller is switched off.

Controller Performance

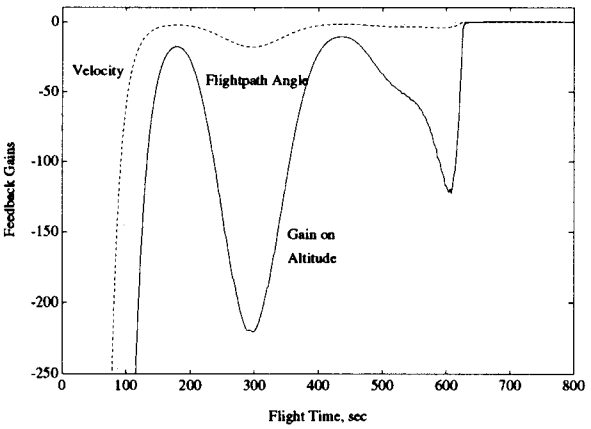

Figure 3: Feedback gains vs. time. Data points are obtained by successive solution of the algebraic Riccati equation.

Preliminary entry conditions of the Space Mail capsule have been published in previous reports[1,2,11]. After a Keplerian transfer, the capsule is assumed to reach the atmosphere at 120 km altitude and an earth-relative flight path angle of −2.8 degrees. In order to model entry condition dispersions, the transfer orbit is represented as a Hohmann ellipse[14] with a fictitious perigee altitude of −200 km and a perigee argument of 170 degrees. Given an orbit inclination of 28.5 degrees, this transfer results in an entry position with a maximum geodetic latitude of 28.5 degrees. This agrees with mission plans to retrieve the capsule on the Canary Islands (west 16°, north 28°). The Hohmann transfer is induced by a single, instantaneous deorbit impulse opposing to the orbit velocity. Entry condition offsets are modeled by perturbing the required deorbit impulse, which leads to nominal entry conditions, by up to −10 per cent. The resulting perturbed entry conditions are listed in Table 2.

The atmosphere density data for nominal flight conditions is taken from the U.S. 1976 Standard Atmosphere[19]. To simulate atmospheric disturbances during reentry flight, the density values are changed to data derived from measurements on Space Shuttle flights with north latitude[20] (STS-9 and STS-17). This Shuttle-derived density profile is up to 50 per cent lower than the U.S. Standard Atmosphere between 120 km and 40 km altitude.

For the numerical simulation of the Space Mail capsule, the following constant vehicle parameters

Table 2: Nominal and off-nominal entry conditions for the Space Mail capsule. Off-nominal entry conditions result from a 10% larger or smaller deorbit impulse. The transfer orbit is modeled as a Hohmann transfer induced by a single, instantaneous deorbit impulse opposing orbit velocity. For entry at 28.5 latitude (Canary Islands), the required perigee argument of the transfer orbit is 170 degrees. Longitude is computed with respect to the nominal entry position.

Impulse Perturbation	+10%	0	−10%
Altitude,km	120	120	120
Velocity,m/s	7422.5	7440.3	7458.3
Flight Path Angle,deg	−3.30	−2.97	−2.60
Longitude,deg	−7.23	0	9.01
Latitude,deg	28.1	28.5	28.4
Heading Angle,deg	5.20	1.76	−2.56

are assumed[1]: a mass of 80 kg, an aerodynamic surface of 0.9 square meters, a drag coefficient of 0.35, and a lift-to-drag ratio of 0.52. Uncertainties of the actual lift-to-drag ratio are estimated at ±4 per cent. Thus, to model vehicle design uncertainties, the lift-to-drag ratio is varied between 0.50 and 0.54.

For the following simulation results, reference trajectories are chosen with a constant control input of 30, 60, and 45 degrees bank angle, respectively. Given nominal entry conditions and nominal parameter values, the 45 degree trajectory is chosen as the design trajectory for the controller. Although this set of trajectories is chosen arbitrarily, it agrees with Space Mail design specifications. With constant bank angles of 60 degrees or lower, the capsule develops enough vertical lift so that the aerodynamic deceleration does not exceed the desired limit of 3g's. A bank angle of constant 45 degrees also provides maximum lateral reach[13,14].

A block diagram schematic of the simulated control system is shown in Fig. 4. The reduced-order regulator receives feedback of the state errors in altitude, velocity, and flight path angle. With these offsets, the controller computes the necessary change in bank angle. A saturation block limits the bank angle input to a range from 0 to 90 degrees. Thus, neither heading reversals nor negative-lift maneu-

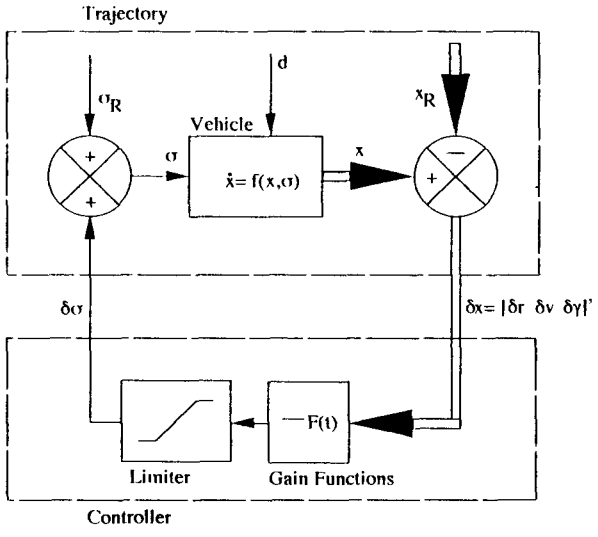

Figure 4: Block diagram schematic of the state feedback regulator system. The non-linear equations of motion are contained in the Vehicle block. Time-varying parameter of the system is the atmospheric density, $d(t)$. The controller, $\mathbf{F}(t)$, the state errors, $\delta\mathbf{x}$ and commands a change in bank angle, $\delta\sigma$. The bank angle input,σ, is limited to range from 0 to 90 degrees.

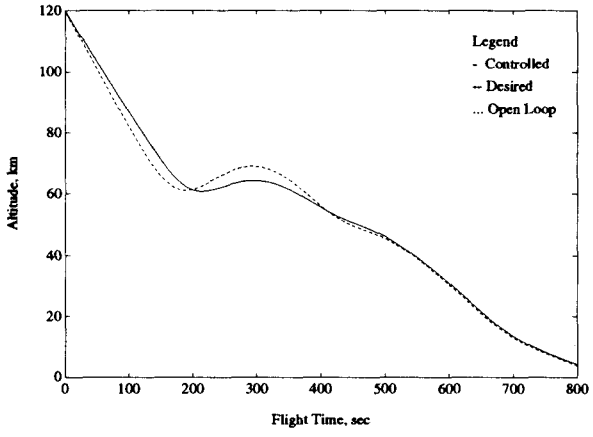

Figure 5: Altitude time response of the feedback regulator system to entry conditions resulting from a 10% smaller deorbit impulse. Simultaneously the vehicle's lift-to-drag ratio is increased to 0.54 from the nominal 0.52. The reference trajectory (dashed line) and the open-loop response (dotted line) are plotted for comparison.

vers are permitted. The response of the system to a set of entry conditions is integrated numerically in the time-domain using the system analysis program Simulink[21].

Figures 5 to 7 show the time responses of altitude, velocity, and flight path angle due to a 10% lower deorbit impulse. Simultaneously, the lift-to-drag ratio of the controlled vehicle is increased by 4% to 0.54. The controller smoothly counteracts the overspeed and also approaches the desired histories of altitude and flight path angle. The controlled vehicle stays close to the desired trajectory after circa 400 seconds. The load factor experienced by the controlled vehicle (see Fig. 8) does not differ greatly from the values on the desired path.

A different case with opposite conditions is presented in Figs. 9 to 11. The plots show the time responses of altitude, velocity, and flight path angle due to a 10 per cent higher deorbit impulse, resulting in a lower entry speed and a shallower flight path angle (see Table 2). At the same time,

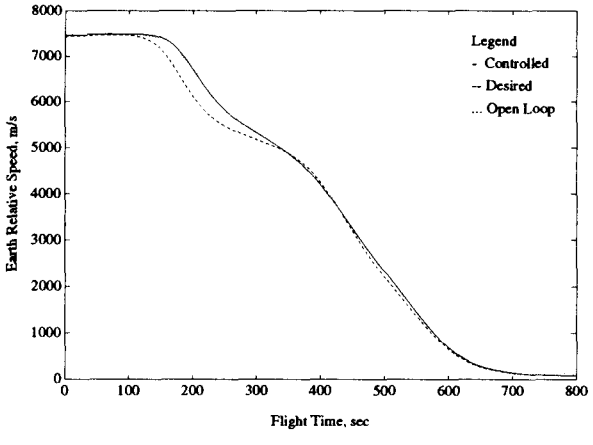

Figure 6: Velocity time response of the feedback regulator system to entry conditions resulting from a 10% smaller deorbit impulse. Simultaneously the vehicle's lift-to-drag ratio is increased to 0.54 from the nominal 0.52.

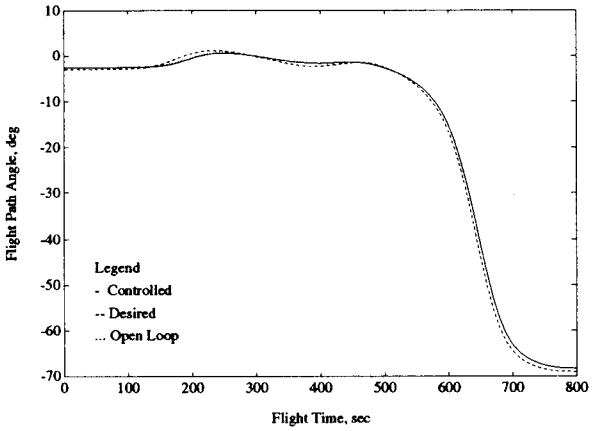

Figure 7: Flight path angle time response of the feedback regulator system to entry conditions resulting from a 10% smaller deorbit impulse. Simultaneously the vehicle's lift-to-drag ratio is increased to 0.54 from the nominal 0.52.

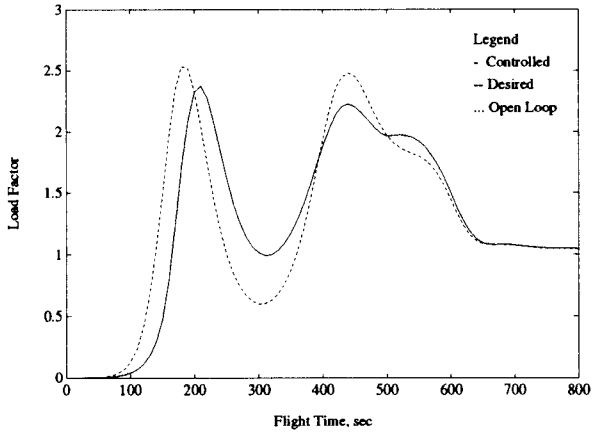

Figure 8: Load factor time response of the feedback regulator system to entry conditions resulting from a 10% smaller deorbit impulse. Simultaneously, the vehicle's lift-to-drag ratio is increased to 0.54 from the nominal 0.52.

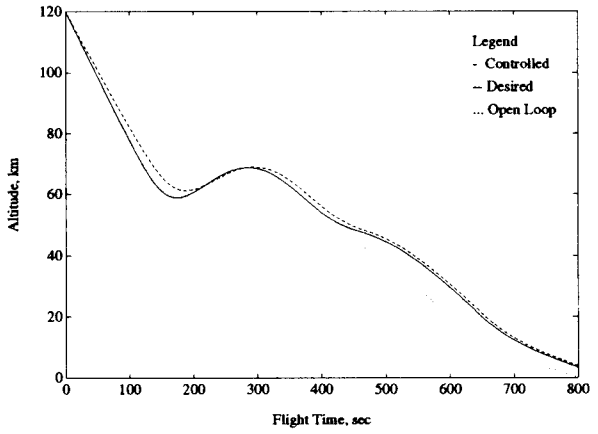

Figure 9: Altitude time response of the feedback regulator system to entry conditions resulting from a 10% larger deorbit impulse. Simultaneously the vehicle's lift-to-drag ratio is decreased to 0.50 from the nominal 0.52.

the lift-to-drag ratio of the controlled vehicle is decreased by 4 per cent to 0.50. Again, the controller is able to counteract these offsets and guide the vehicle to the desired trajectory. The controlled vehicle's speed increases when compared to the uncontrolled response and approaches the desired trajectory asymptotically. Also, altitude and flight path angle response approach the desired within satisfactory steady state error limits. The control action has lowered the load factor response of the controlled vehicle (see Fig. 9), but the peak load on the controlled path exceeds the desired peak value.

The time histories of the bank angle input for the two above cases are plotted in Fig. 13. One can see that the transients for the opposite speed and angle offsets are mirror images. In both cases, the bank angle response is a smooth function that undergoes one oscillation at a maximum rate of approximately 1 degree per second.

Strictly speaking theoretically, a computed gain schedule is only valid for the particular trajectory for which it is designed. However, for practical applications, it is of interest how the same gain functions perform on a reference trajectory other than the design trajectory. The following preliminary test results show that the gain schedules designed for the 45 degree reference trajectory (see Fig. 3) do well also on trajectories with constant 30 and 60 degrees bank angle.

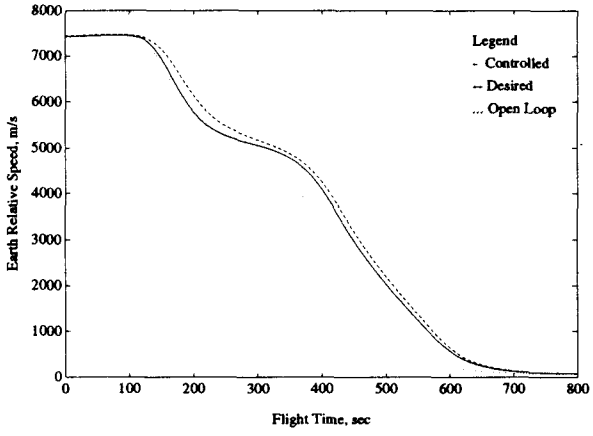

Figure 10: Velocity time response of the feedback regulator system to entry conditions resulting from a 10% larger deorbit impulse. Simultaneously the vehicle's lift-to-drag ratio is decreased to 0.50 from the nominal 0.52.

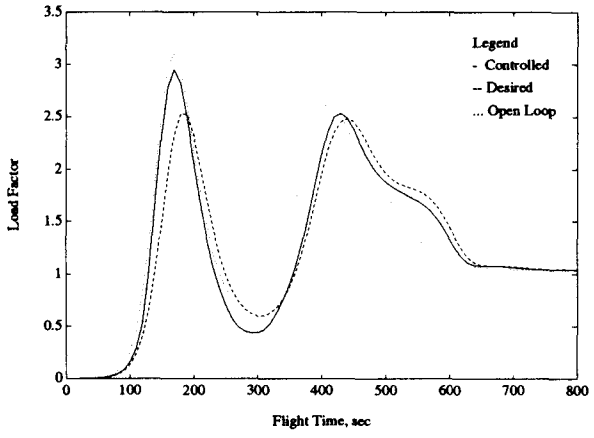

Figure 12: Load factor time response of the feedback regulator system to entry conditions resulting from a 10% larger deorbit impulse. Simultaneously, the vehicle's lift-to-drag ratio is decreased to 0.50 from the nominal 0.52.

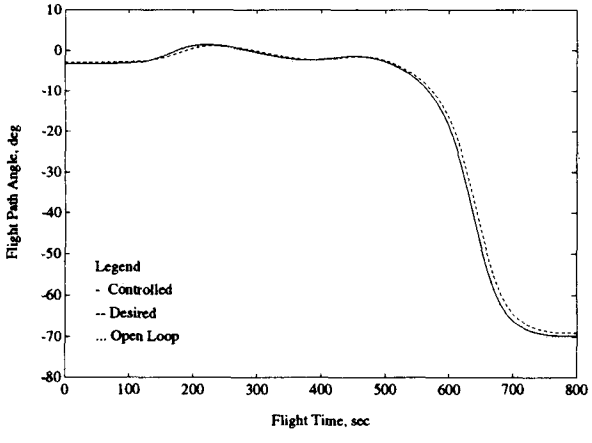

Figure 11: Flight path angle time response of the feedback regulator system to entry conditions resulting from a 10% larger deorbit impulse. Simultaneously the vehicle's lift-to-drag ratio is deØcreased to 0.50 from the nominal 0.52.

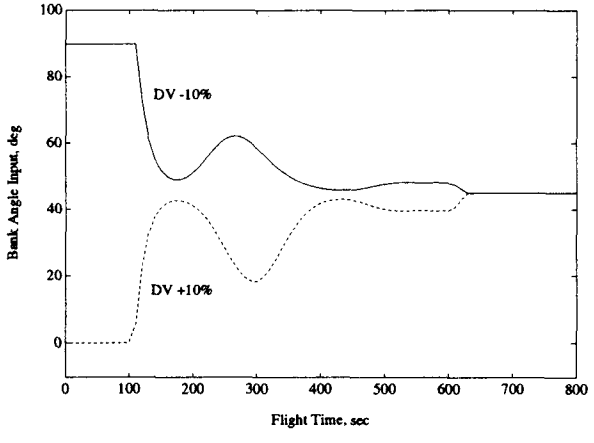

Figure 13: Bank angle input time response as commanded by the controller for a 45 degree reference trajectory. Response of the feedback regulator system to entry conditions resulting from ±10% deorbit impulse perturbations. Simultaneously, the vehicle's lift-to-drag ratio is increased to 0.54 or decreased to 0.50 from the nominal 0.52, respectively. ("Worst case" combination)

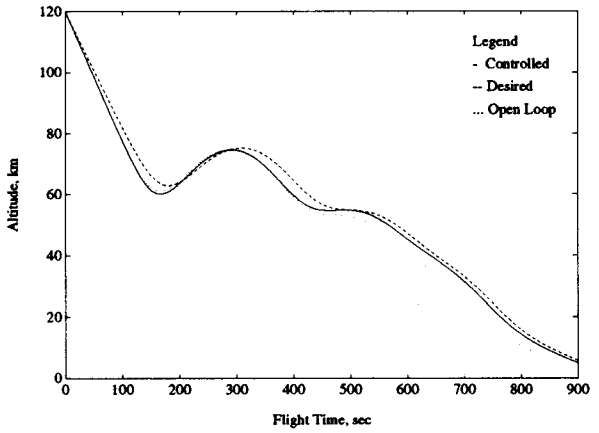

Figure 14: Altitude time response of the feedback regulator system to entry conditions resulting from a 10% larger deorbit impulse. The reference trajectory is computed for constant 30 degrees bank angle, while the controller gains are designed for a 45 degree reference trajectory.

Figures 14 to 18 show the time responses of altitude, velocity, and the bank angle input due to a 10 per cent larger deorbit impulse on a 30 degree reference trajectory. The vehicle approaches the desired trajectory eventually, but slower and later than on the 45 degree reference (Figs. 9 and 10). However, on a 60 degree reference with a 10 per cnet smaller deorbit impulse (Figs. 16 and 17), the performance of the controller is comparable to operation on the 45 degree reference (Figs. 5 and 6).

These results demonstrate that the proposed state feedback controller, which is designed for a particular reference trajectory, does not lose control over the vehicle when it is directed to a different reference trajectory. For practical applications, this implies that the number of gain schedules that need to be stored aboard the spacecraft may be limited without sacrificing performance. Also, a state feedback controller becomes eligible for combination with onboard prediction methods.

Conclusions

As opposed to previously suggested predictor schemes, this paper presents reentry guidance for the Space Mail capsule using a linear state feedback path following controller. The controller design principle is summarized and simulation results

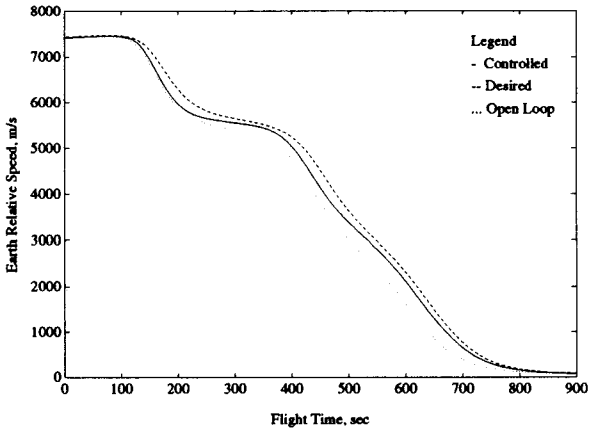

Figure 15: Velocity time response of the feedback regulator system to entry conditions resulting from a 10% larger deorbit impulse. The reference trajectory is computed for constant 30 degrees bank angle, while the controller gains are designed for a 45 degree reference trajectory.

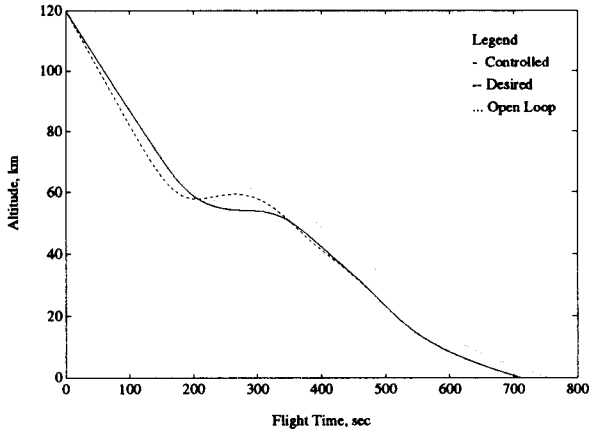

Figure 16: Altitude time response of the feedback regulator system to entry conditions resulting from a 10% smaller deorbit impulse. The reference trajectory is computed for constant 60 degrees bank angle, while the controller gains are designed for a 45 degree reference trajectory.

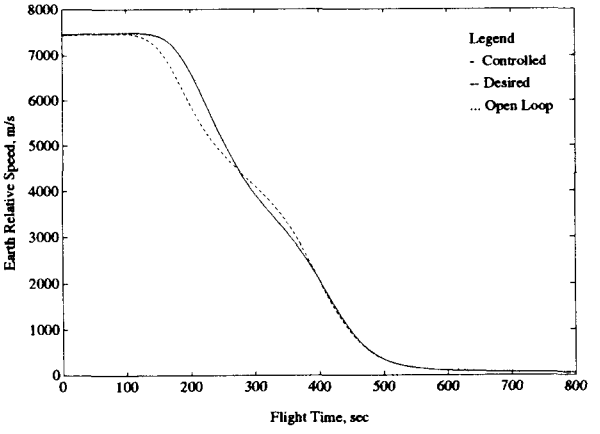

Figure 17: Velocity time response of the feedback regulator system to entry conditions resulting from a 10% smaller deorbit impulse. The reference trajectory is computed for constant 60 degrees bank angle, while the controller gains are designed for a 45 degree reference trajectory.

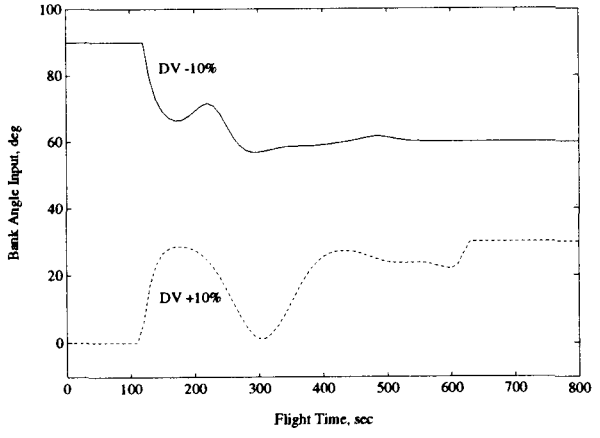

Figure 18: Bank angle input time response as commanded by the controller for a 30 degree and 60 degree reference trajectory. Response of the feedback regulator system to entry conditions resulting from ±10% deorbit impulse perturbations. The controller gains are designed for a 45 degree reference trajectory.

of the performance of the designed feedback controller are presented.

The results in this paper show that the proposed controller responds effectively to entry condition offsets resulting from deorbit impulse perturbations of ±10 per cent. Simultaneously, the controller is capable of adjusting to lift-to-drag ratio variations of ±4 percent as well as atmospheric disturbances. The presented results show that the performance of the controller is satisfactory even on reference trajectories that are different from the design trajectory.

We plan to apply the path control system presented here to advanced guidance laws including terminal control. A path controller is to improve the accuracy of the pursued trajectory and to reduce landing site dispersions.

Acknowledgments

We gratefully acknowledge the helpful discussion with Dr. Ulrich M. Schöttle of the University of Stuttgart Institute of Space Systems.

References

[1]M. H. Aenishanslin. *Space Mail Feasibility Study.* Columbus Preparatory Programme Report COL-TN-AS-0050. Les Mureaux, France: Société Nationale Industrielle Aérospatiale, November 1986.

[2]U. Schöttle et al. "Conceptual Study of a Small Semiballistic Reentry Experiment Vehicle." International Astronautical Federation. Proceedings of the 41st Congress, Report IAF-90-163, Dresden, Germany, 6–12 October 1990.

[3]R. C. Wingrove. "A Survey of Atmosphere Reentry Guidance and Control Methods." *AIAA Journal*, Vol. 1, No. 9, September 1963.

[4]R. C. Duncan. "Guidance and Control for Atmospheric Entry." Vol. II. *Re-Entry and Planetary Entry Physics.* ed. W. H. Loh. New York: Springer-Verlag, 1968.

[5]J. C. Harpold, C. A. Graves. "Shuttle Entry Guidance." *Journal of the Astronautical Sciences*, Vol. 26, No. 3, July 1979.

[6]E. J. Cramer et al. "NLP Reentry Guidance: Developing a Strategy for Low L/D Vehicles." AIAA Paper 88-4123-CP, 1988.

[7]L. Skaslecki, M. Martin. "General Adaptive Guidance Using Nonlinear Programming Constraint

Solving Methods (FAST)." AIAA Paper 91-2820-CP, 1991.

[8]R. H. Battin. *Astronautical Guidance.* New York: McGraw-Hill, 1964.

[9]W. Beier, H. Kallerhof. "Positionsbestimmung für Raumfahrzeuge mit dem Satellitennavigationssystem GPS." [Positioning of Space Vehicles with the Satellite Navigation System GPS] *Elektrisches Nachrichtenwesen,* Vol. 62, No. 1, 1988.

[10]T. Jacob, M. Dieroff. "Integrated Navigation for Approach Guidance Using Differential GPS." American Institute of Navigation. Proceedings of the 1990 GPS Conference, Colorado Springs, September 1990.

[11]A. J. Roenneke, P. J. Cornwell. "Trajectory Control for a Low-Lift Maneuverable Reentry Vehicle." AIAA Paper 92-1146-CP, 1991.

[12]A. Miele. *Flight Mechanics.* Reading, Mass: Addison-Wesley, 1962.

[13]N. X. Vinh. *Optimal Trajectories in Atmospheric Flight.* New York: Elsevier, 1981.

[14]A. E. Bryson, Y. Ho. *Applied Optimal Control.* New York: Hemisphere Publishing, 1975.

[15]Paris D. et al. *Guidance and Control for Moderate Lift/Drag Reentry.* Contract 9359/91/NL/JG. Noordwijk, The Netherlands: European Space and Technology Center, 1992.

[16]A. J. Roenneke. *Trajectory Control for a Low-Lift Maneuverable Reentry Vehicle Using State Feedback.* Master of Science Thesis. Terre Haute, Ind: Rose-Hulman Institute of Technology, 1991.

[17]H. Kwakernaak, R. Sivan. *Linear Optimal Control Systems.* New York: Wiley-Interscience, 1972.

[18]A. J. Laub, J. N. Little. *Control System Toolbox.* For Use with Matlab. User's Guide. Natick, Mass: The MathWorks Inc., August 1986.

[19]U.S. National Oceanic and Atmosperic Administration. *U.S. Standard Atmosphere 1976.* Report NOAA-S/T 76-1562. Washington: U.S. GPO, 1976.

[20]J. D. Gamble, J. T. Findlay. "Shuttle-Derived Densities in the Middle Atmosphere." AIAA Paper 88-4352-CP, 1988.

[21]The MathWorks, Inc. *Simulab. A Program for Simulating Dynamic Systems.* User's Guide. Natick, Mass: The Company, July 1991.